

Effect of Wall Height on Stresses Distribution in a Earth Wall Reinforced with Geosynthetics

Amin Zivari¹, Morteza Tasdighi²

¹Phd Student, Geotechnic, Civi Engineering Dept., Islamic Azad University, Isfahan, Iran

²Graduated M.Sc., Geotechnic, Shams Higher Education Institute, Gonbad, Iran

ABSTRACT

The superiority of geosynthetics over other reinforcements has led to the introduction of retaining walls reinforced with geosynthetics as an important option in the design of retaining walls. The lack of problems such as corrosion, rust, better engagement with materials, and ease of implementation are advantages of this approach. Soil retaining walls reinforced with geosynthetics are generally designed based on the limit equilibrium method. In this method, the effect of factors such as specific boundary conditions, tough reinforcement, and type of facing are not considered. The present study used the finite element method with PLAXIS 2D software to develop several 2D models under plane strain conditions. The results showed that horizontal displacement and vertical settlement were strongly influenced and their values increased dramatically as wall height increased. The maximum axial forces created in the reinforcement and the lateral soil pressure increased as the wall height increased.

Keywords: Reinforced earth wall, finite element, numerical analysis, wall height.

1. INTRODUCTION

Reinforced soil is a material composed of soil and reinforced elements. In this complex system, soil grains are responsible for bearing compressive forces and reinforced elements increase soil shear resistance by tolerating tensile stress, therefore, the most important structural element for increasing soil tensile strength is the reinforced element. Material characteristics such as length, spacing, and density are essential design factors for reinforced soil. Methods of designing and constructing a reinforced soil wall together with its basic rules have overshadowed its design so that the concept of soil reinforcement has been broadly studied. [Bolton, 1991] [Ingold, 1982] [Jewell, 1991] [Mitchel, 1982] [Schlosser and uran, 1980-1983] [Schlosser, 1990] [Gassler, 1991].

Reinforced soil is a slope or retaining wall that is reinforced while forming an embankment. Compared to gravity or concrete walls, reinforced retaining soil walls have greater flexibility, show good behavior under a variety of loads, and can tolerate relatively large deformations. Most current methods of stability analysis of reinforced soil structures assume that the wall shell plays an important role in the overall stability of the wall and do not consider the effect of rigidity of the shell; however, the basic goal for design of the shell is to prevent erosion of the slope and to keep the front layer in place. The design of such walls is conservative estimate [Vidal,H. 1978]. The present study used numerical modeling of finite elements using PLAXIS 2D software to address the effect of the height of a reinforced soil wall on deformation, lateral pressure of the embankment, and axial forces of the reinforcements behind the wall.

2. NUMERICAL MODELING

Figure 1 shows the cross-section geometry of the models. Walls w-H6, w-H10, w-H15, and w-H20 had heights of 6,10, 15, and 20 m, respectively, with a common facing thickness of $t = 20$ cm. To investigate the effect of wall height, wall thickness was held constant and height was increased. After selecting the wall height, a width should be selected that prevents geometric boundary effects from influencing analysis; thus, the wall width (sum of reinforced and unreinforced zone) was assumed to be approximately 5 times its height. A rigid foundation was selected to allow modeling at a width that is greater than the wall width. This was done to eliminate the effect of foundation type in the analysis. It was assumed that the wall was built on a rigid foundation of high strength with behavior that did not affect the wall (minimal effect of foundation horizontal and vertical deformations on wall horizontal displacement and vertical settlement).

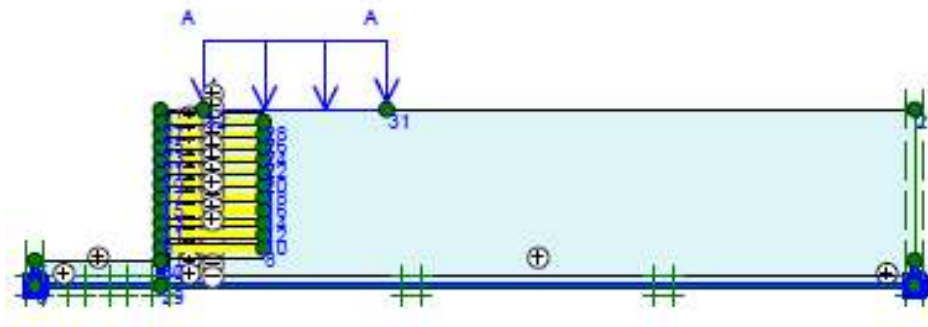


Fig. 1. Overview of model geometry

3. MATERIALS

Embankments generally maintain an average relative density; thus, the modeled embankments were of average density. The Mohr-Coulomb (Elastoplastic) model was used for the embankment materials. Geogrids were used between the soil layers, thus, it was necessary to enter their specifications into the PLAXIS 2D software. Geogrid is a tensile element and the type associated with EA parameters was introduced into the program. reinforcement length for static analysis should be $L = 0.7H$, where H is the wall height (FHWA, 2001).

Because all analyses were in static form, the geogrid reinforcement length was set at 0.7 H in all models. The soil-wall and reinforcement-soil interaction coefficients were set at $R = 0.67$ and $R = 0.9$, respectively [Budhu, M. 2000, Bergado, D.T., 2003]. To simplify the model, the type of reinforced soil in the area and behind it were considered to be identical. The wall foundation and facing had a specific gravity of 2.4 ton/m³ and Poisson's ratio of 0.2. Specifications of concrete elasticity modulus were accordance with recommendations by the American Concrete Institute, $E = 15100\sqrt{f_c}$ [ACI 318 R-02].

To determine the input parameters of the structural members such as modulus of elasticity for the shell and foundation, $E = 2.6 \times 10^5 \text{ kg/cm}^2$ was computed for $f_c = 300 \text{ kg/cm}^2$ and the Poisson's ratio of the concrete shell and foundation was set at $\nu = 0.2$. An elastic model was employed for the shell and foundation materials. The profile of the materials are shown in Tables 1, 2, and 3.

Table 1. Wall foundation and facing properties

Material	Poisson's ratio (ν)	Unit Weight (γ) KN/m ³	Modulus of elasticity (E_s) Mpa
Foundation	0.2	24	2.6
Facing	0.2	24	2.6

Table 2. Profile of the embankment materials

Symbol	W-H6	W-H10	W-H15	W-H20
Geogrid length (L)m	4.2	7	10.5	14
Axial stiffness (EA)kN/m	2000	2000	2000	2000
Vertical distances of reinforcements (Sv)m	0.5	0.5	0.5	0.5

Table 3. Properties of a geogrid-type reinforcement

Symbol	W-H6	W-H10	W-H15	W-H20
Angle of internal friction (ϕ°)	36	36	36	36
Angle of dilation (ψ°)	6	6	6	6
Special Weight (γ) KN/m ³	18	18	18	18
Modulus of Elasticity (E_s) Mpa	35	35	35	35
Poisson's ratio (ν)	0.3	0.3	0.3	0.3
Adherence (C)KN/ m ²	0.2	0.2	0.2	0.2

4. LOADING

Given the failure wedge position in the reinforced soil walls with concrete facing according to Figure 2 [Schlosser, F 1990], a distance of $H = 0.3$ from the edge of the wall was maintained to prevent overloading from entering the driving range. Three loading modes were considered; mode 1 was without overloading and mode 2 had overloading equivalent to a traffic length of 6 m. In the design method proposed by Kutara et al. [Kutara, K., 1980], the traffic load was considered to be equivalent to the static load. The equivalent road load was set at 12 kN/m^2 and was statically applied to the model. Mode 3 assumed overhead to be a conventional 3-story building of 30 kN/m^2 and a length of 10 m.

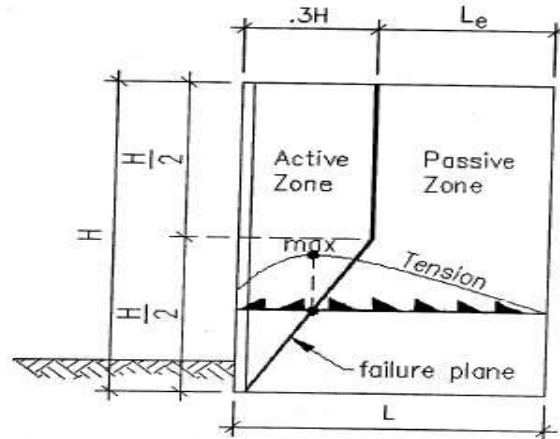


Fig. 2. Slip surface position in the reinforced soil retaining walls

5. MESHING AND MODEL ANALYSIS

The finite element model used to model plane strain. PLAXIS provides 2 triangular elements of 15 and 6 nodes. Because the 15-node elements provide more accurate results, they were employed for analysis. After meshing, the model was analyzed using plastic analysis in PLAXIS. The analytic phases were defined for modeling the construction process. It was assumed that the embankment behind the wall was created in one stage to allow examination of the wall behavior after construction.

6. RESULTS OF ANALYSIS

a. Horizontal and vertical deformations

Figures 3 to 5 show normalized graphs of horizontal displacement ($\delta x/H$) versus wall height (h/H). The maximum horizontal displacement was marked at the wall crown for walls w-H6, w-H10, and w-H15 and are 0.7-0.8 H for wall w-H20. As seen, as wall height increased, maximum horizontal displacement (δx_{max}) changed from linear to parabolic mode. The position of maximum horizontal displacement moved from the upper to middle levels as wall height increased. Increasing the wall height from 6 to 10 m increased maximum displacement 3-fold (δx_{max}) and 2.6-fold at $qs = 0$ and $qs = 30 \text{ kN/m}^2$, respectively. Increasing the wall height from 6 to 15 m, increased maximum displacement 6.9-fold (δx_{max}) and 5.6-fold for $qs = 0$ and $qs = 30 \text{ kN/m}^2$, respectively. Increasing the wall height from 6 to 20 m, increased the maximum displacement 11.4-fold (δx_{max}) and 9.3-fold for $qs = 0$ and $qs = 30 \text{ kN/m}^2$ respectively.

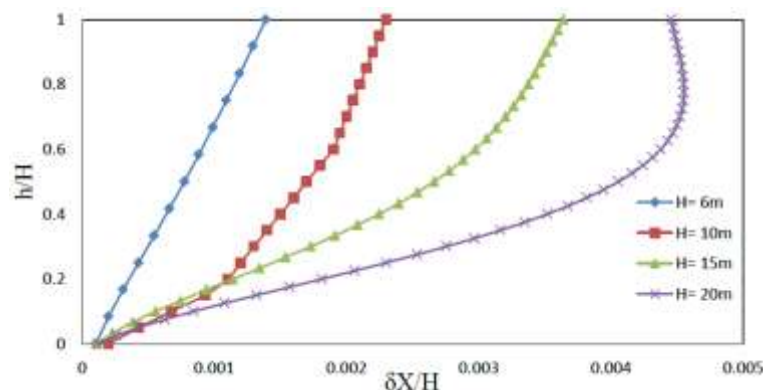


Fig. 3. Normalized diagram of horizontal displacement ($\delta x/H$)-wall height (h/H) at different facing heights for $qs = 0 \text{ kPa}$

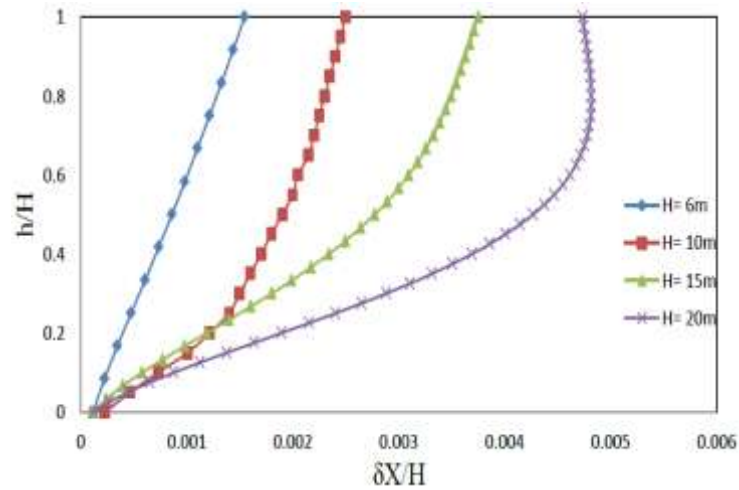


Fig. 4. Normalized diagram of horizontal displacement ($\delta x/H$)-wall height (h/H) at different facing heights for $q_s = 12$ kPa

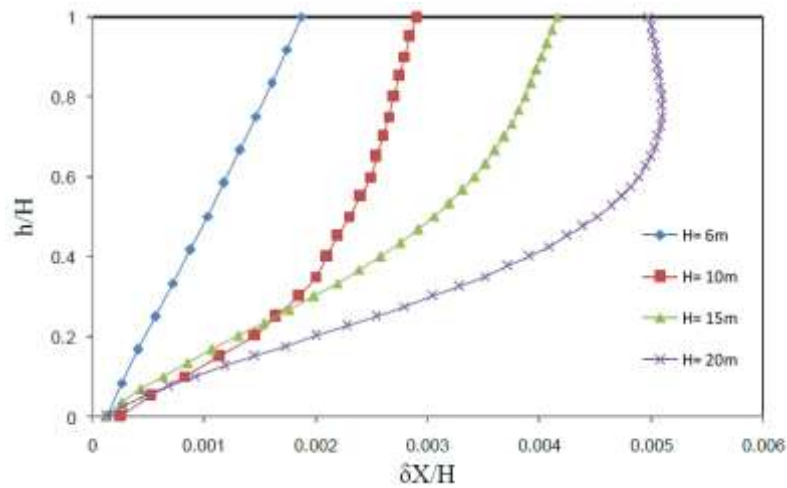


Fig. 5. Normalized diagram of horizontal displacement ($\delta x/H$)-wall height (h/H) at different facing heights for $q_s = 30$ kPa

Increasing the wall height from 6 m to 10 m increased settlement 2.75-fold and 5.5-fold in the reinforced and unreinforced limits for $q_s = 0$, respectively, and increased settlement 2.7-fold and 3.2-fold for $q_s = 30$ kN/m², respectively. Increasing wall height from 6 to 15 m increased settlement 6.25-fold and 8-fold in the reinforced and unreinforced limits for $q_s = 0$, respectively and 4.7-fold and 5.5-fold for $q_s = 30$ kN/m², respectively. Increasing wall height from 6 to 20 m increased settlement 10.5-fold and 21-fold in the reinforced and unreinforced limits for $q_s = 0$, respectively and 8.6-fold and 10-fold for $q_s = 30$ kN/m², respectively. It should be noted that the lengths and axial stiffness of the reinforcements can be increased and their vertical spacing decreased in weak areas to control and reduce the horizontal displacement and vertical settlement.

b. Reinforcement tensile force

Figures 6 to 8 show the normalized graphs of maximum tensile force in the reinforcements ($T_{max}/K_{ay}HS_v$) at different points along the height of the wall (h/H). The maximum tensile forces in the reinforcements were in the ranges of 0.3-0.4 H, 0.2-0.3 H, 0.2-0.3 H, and 0.15-0.3 H for walls w-H6, w-H10, w-H15, and w-H20, respectively. The diagrams indicate that for a fixed height, an increase in overhead increased the reinforcement tensile force. As the wall height increased, the incremental trend of the reinforcement tensile forces became more evident. The maximum increase (T_{max}) was 7% to 11% for a fixed height at $q_s = 0$ -30 kPa; it was 45% to 47% for $H = 6$ -20 m at a similar q_s . As seen, the ascending trend of reinforcement tensile force changed to a descending trend at the lower levels of the wall. The reason for this is that the connection of the shell clamped to the foundation, restrictions in deformation, and the subsequent failure of complete mobilization of the soil shear force within the bottom limits of the wall.

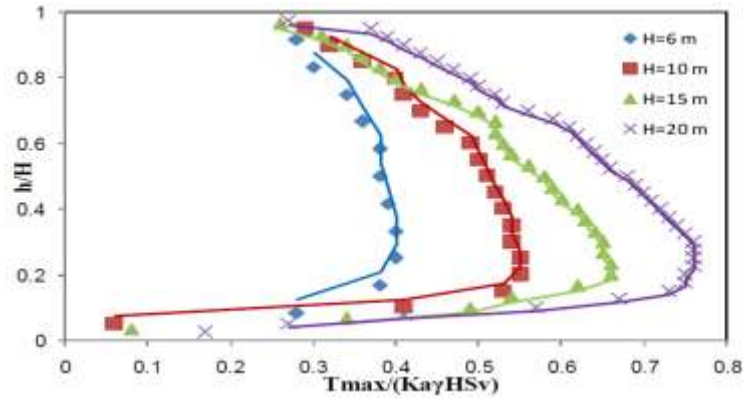


Fig. 6. Normalized graph of reinforcement maximum tensile force ($K_a\gamma HS_v / T_{max}$) (h/H for different facing heights at $q_s = 0$)

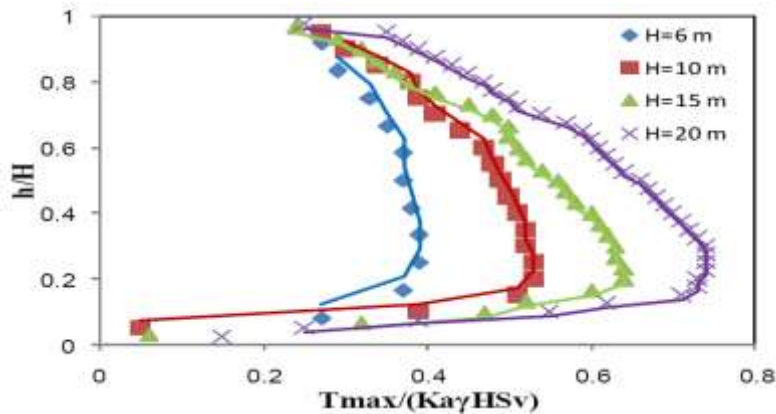


Fig. 7. Normalized graph of reinforcement maximum tensile force ($K_a\gamma HS_v / T_{max}$) (h/H for different facing heights at $q_s = 12\text{kPa}$).

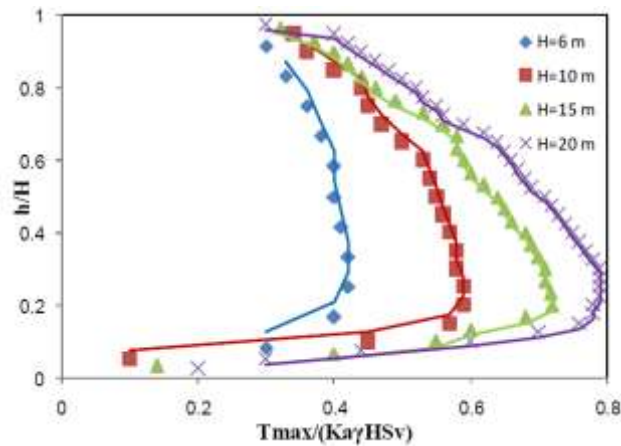


Fig. 8. Normalized graph of reinforcement maximum tensile force ($K_a\gamma HS_v / T_{max}$) (h/H for different facing heights at $q_s = 30\text{kPa}$).

c. Lateral soil pressure

Figures 9 to 11 show the normalized charts of lateral soil pressure $\sigma_h/(\gamma H)$ versus wall height (h/H). The graphs show that at a fixed height an increase in q_s , will decrease the lateral soil pressure behind the shell in response to an increase in lateral deformation caused by the increase in q_s . An increase of 6 to 20 m in the wall height caused the lateral soil pressure to change from a at rest to a active Rankin state. As height increased, a further increase in lateral deformation causes active Rankin pressure to predominate over the wall.

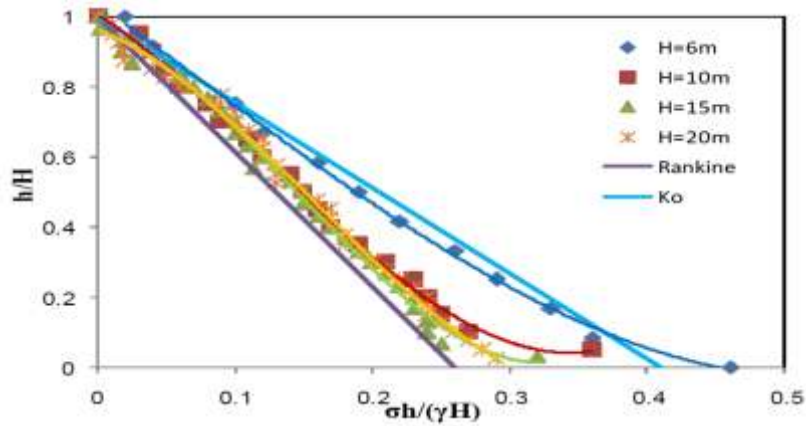


Fig. 9. Normalized graph of lateral soil pressure $\sigma_h/(\gamma H)$ -wall height at different facing heights for $q_s = 0$

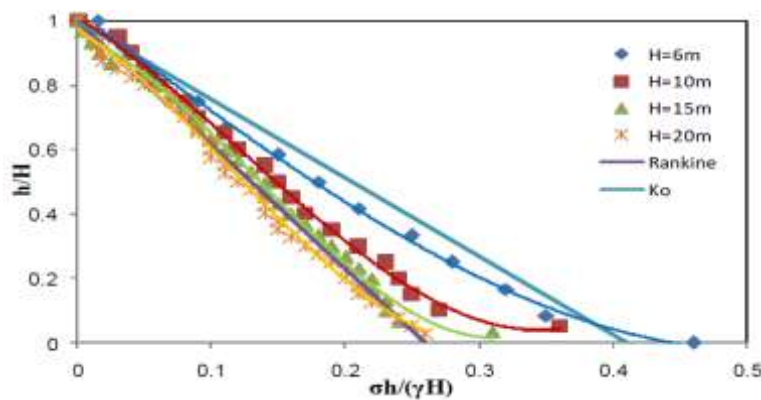


Fig. 10. Normalized graph of lateral soil pressure $\sigma_h/(\gamma H)$ -wall height at different facing heights for $q_s = 12 \text{ kPa}$

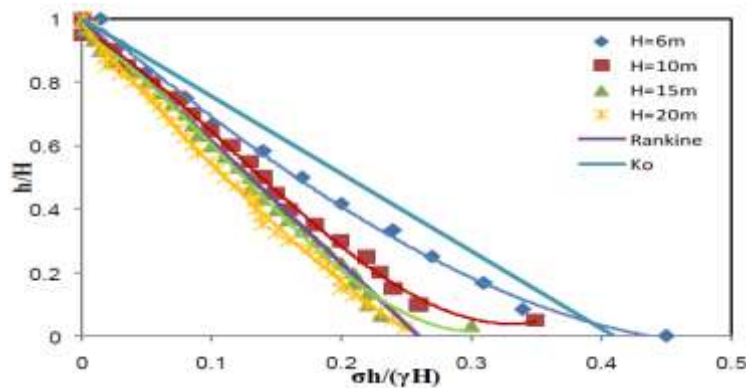


Fig. 11. A normalized graph of lateral soil pressure $\sigma_h/(\gamma H)$ -wall height for the different heights of the facing for $q_s = 30 \text{ kPa}$

7. CONCLUSION

The results of this research indicate that increasing the wall height:

- Changed the position of maximum horizontal displacement from the upper to middle levels.
- Dramatically increased the horizontal displacement and vertical settlement. To prevent exceedence of allowed limits, measures such as increasing the stiffness of the reinforcements, increasing their lengths, or decreasing the vertical distance between them should be carried out.
- Produced an increasing trend in maximum. The maximum axial forces values (T_{max}) created in the reinforcement increased.
- Caused the lateral soil pressure to change from at rest to a active state and Rankin active pressure conditions to prevail over the wall.

REFERENCES

- [1]. Bergado, D.T., Youwai, S., Teerawattanasuk, C., and Visudmedanakul, P. (2003), "The Interaction Mechanism and Behavior of Hexagonal Wire Mesh Reinforced Embankment with Silty Sand Backfill on Soft Clay," *Computers and Geotechnics*, Vol. 30, pp. 517-534.
- [2]. Bolton, M.J. 1991. Reinforced soil: laboratory testing and modeling, S-O-A Report, Performance of Reinforced Soil structures, McGown et al. (ed.). Thomas Telford, pp.287-298.
- [3]. Budhu, M. 2000, *Soil Mechanics and Foundations*, John Wiley and sons, Inc.
- [4]. FHWA (2001), *Mechanically Stabilized Earth Walls and Reinforced Soil Slopes. Design and Construction Guidelines*. FHWA-NHI-00-043, Federal Highway Administration, US Department of Transportation, Washington D.C.
- [5]. Gassler, G. 1991. In-situ techniques of reinforced soil; S-O-A Report, Performance of Reinforced Soil Structures, McGown et al. (ed.), Thomas Telford, pp.185-196.
- [6]. Ingold, T.S. 1982. *Reinforced earth*, Thomas Telford Ltd, London.
- [7]. Jewell, R.A. 1991. Application of revised design charts for steep reinforced slope, *Geotextiles and geomembranes* 10, pp.203-233.
- [8]. Kutara, K., Miki, H., Mashita, Y. and Seki, K. (1980) Settlement and countermeasures of the road with low embankment on soft ground, *Tech. Reo. Of Civil Eng., JSCE*, 22(8), 13-16 (In Japanese).
- [9]. Mitchell, J.K. 1982. Soil improvement, S-O-A Report for Session 12, Proc. Int. Conf. on SMFE, Stockholm, Vol.4, pp.509-565.
- [10]. Schlosser, F. and Juran, I. 1983. Behaviour of reinforced earth retaining Walls from model studies, Chapter 6, 3.3.3 Modelling the Facing, *Developments in SMFE-1*, Applied Science Publishers, pp.197-229.
- [11]. Schlosser, F. 1990. Mechanically stabilized earth retaining structures in Europe, *Design and Performance of Earth Retaining Structures*, Geotechnical Special Publication No.25, ASCE, Lambe and Hansen (ed.), pp.347-378.
- [12]. Vidal, H. 1978. The development and future of Reinforced Earth, Keynote Address, Proc. of Sympo. on Earth Reinforcement, ASCE, pp.1-61 Schlosser, F. (1990).
- [13]. Mechanically stabilized earth retaining structures in Europe, *Design and Performance of Earth Retaining Structures*, Geotechnical Special Publication No.25, ASCE, Lambe and Hansen (ed.), pp.347-378.